

Spatial characteristics of the second-order visual pathway revealed by positional adaptation

Paul V. McGraw¹, Dennis M. Levi² and David Whitaker¹

¹Department of Optometry, University of Bradford, Richmond Road, Bradford BD7 1DP, UK

²College of Optometry, University of Houston, Calhoun Boulevard, Houston, Texas 77204-6052, USA

Correspondence should be addressed to P.V.M. (p.v.mcgraw@bradford.ac.uk)

The visual system is thought to process luminance (first-order) and contrast (second-order) information by dedicated cortical streams. To explore the spatial characteristics of the second-order pathway, we examined the effect of adaptation on spatial localization in human subjects. We show that, unlike first-order adaptation, second-order positional adaptation via cortical mechanisms transfers across orientations but not across spatial frequencies. These results support physiological evidence that these two processing streams are distinct and suggest that the cortical mechanism mediating second-order positional adaptation maintains spatial frequency information but sums signals across orientations.

The visual system is adept at detecting, localizing and analyzing objects, regardless of whether they are defined by variations in luminance or by variations in contrast, color, motion or texture. Objects that are defined by variations in luminance (first-order information) are thought to be detected by neurons in the primary visual cortex (area V1) that signal the difference in average luminance between the excitatory and inhibitory regions of their receptive field. Such neurons behave as simple linear filters, computing the linear sum of luminance levels in the different regions¹⁻⁴. Objects defined by variations in contrast or texture (second-order information) are invisible to linear neurons, because the average luminance is the same in the excitatory and inhibitory regions of their receptive fields. Instead, second-order information is thought to be detected by specialized neurons located in cortical areas V1 and V2 (refs. 5-7). Such neurons must perform a nonlinear operation to detect differences in contrast or texture between regions that have the same average luminance. Experimental second-order stimuli (Fig. 1) are commonly composed of a low-frequency envelope superimposed onto a 'carrier' pattern of higher spatial frequency. If the carrier pattern is sufficiently fine—that is, if the spatial extent of luminance variations within the carrier is small relative to the receptive field of the second-order neuron—then the sum of luminance increments and decrements are equal between the excitatory and inhibitory regions. For this reason, cortical neurons with linear receptive fields that are large relative to the carrier's spatial frequency cannot signal the presence of second-order visual stimuli⁸.

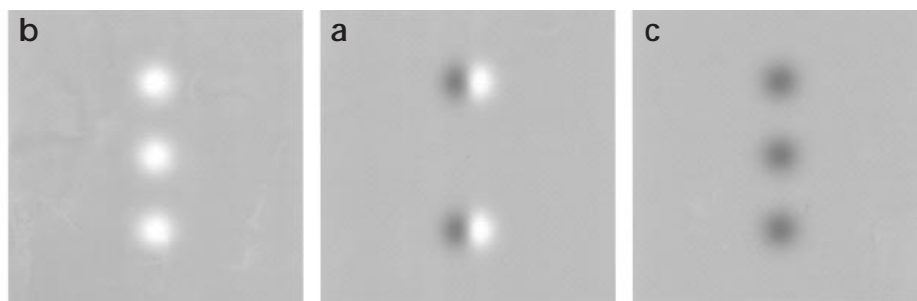
Second-order information is thought to be computed at an early stage in the visual processing stream and then conveyed to dedicated pathways that detect features such as motion and pattern⁹⁻¹⁴. In the current view, the texture elements that define a second-order stimulus are first analyzed by linear neurons tuned to relatively high spatial frequencies, whose output is then subjected to a nonlinear processing step such as rectification. The rectified signal is then conveyed to a second linear filter tuned to a coarser spatial scale. Because sizes of filters before

and after rectification do not overlap, first-order information cannot pass through this sequence; in other words, the second-order filter can detect boundaries defined by texture but not by luminance. This processing stream of filter-rectify-filter has been identified in the striate cortex of cats¹⁵, and is also supported by psychophysical evidence in humans¹⁶⁻¹⁹. In addition, cortical neurons have been identified that respond to second-order visual stimuli of specific orientations²⁰⁻²². Although these neurons also show some selectivity for the orientation of the first-order carrier grating, there is no fixed orientational relationship between the initial and later-stage filters²².

These findings suggest a physiological framework for understanding how second-order stimuli are detected. By pooling information from many neurons tuned to second-order stimuli of the same orientation (but with different preferences for the orientation of the first-order carrier stimuli), a filter could be constructed that could detect second-order contours independent of the texture by which they are defined.

We tested this model psychophysically, using an adaptation protocol and spatial localization task to investigate how information is pooled to allow accurate localization of second-order stimuli. Pattern adaptation occurs through the selective stimulation of discrete subpopulations of neurons that respond to similar image features, and thus it has been widely used to study the processing of first-order information in human vision. It has revealed selectivity to spatial frequency^{23,24}, orientation²⁵, temporal frequency²⁶, color²⁷, motion²⁸ and position²⁹. In a previous study, we showed that adaptation to either first- or second-order adapting stimuli produces large perceived offsets in subsequent test stimuli of the same type (first- or second-order), although little or no crossover effect was found²⁹. Here we used a modified version of the same method to study how first-order orientation information is pooled during the detection of second-order stimuli. Our subjects adapted to second-order stimuli that consisted of blobs of contrast modulation of a carrier grating, and then were tested for errors in localizing

Fig. 1. Demonstration of positional adaptation for first-order stimuli. **(a)** Adapting stimulus; **(b)** test stimulus composed of luminance increments; **(c)** test stimulus composed of luminance decrements. The observer should note that adaptation to **(a)** produces subsequent misalignments in **(b)** and **(c)** of approximately equal magnitude but opposite direction.



target stimuli on gratings of different orientations or spatial frequencies. We found that there is nearly complete transfer of adaptation across orientation, but not across spatial frequency.

RESULTS

The effects documented below may be verified for both first- and second-order stimuli by viewing the demonstration stimuli (Figs. 1 and 2). First, fixate on the small cross at the center of the two anti-symmetric outer blobs in Fig. 1a for 10–15 seconds. A quick gaze shift to the center of Fig. 1b should produce a perceived offset of the central element, despite true physical alignment of the stimulus elements. Effectively, the luminance gradient of the elements in the adapting stimulus shifted the perceived position of the outer, luminance-incremented blobs (test stimulus) in the direction of the adapting gradient, that is, from right to left. If the adapting procedure is repeated and gaze transferred quickly to Fig. 1c, the reader should note a similar offset in the opposite direction. In this case, the outer luminance-decrement blobs of the test stimulus have been shifted in the opposite direction to the luminance gradient in the adapting stimulus, that is, from left to right. The same is also true for second-order stimuli. If the reader fixates the small cross at the center of the adapting stimulus shown in Fig. 2a for 10–15 seconds and then quickly transfers gaze

to the center of Fig. 2b, once again, a perceived offset of the central element should be observed, despite true physical alignment. Like their luminance counterparts, contrast increments and decrements (Fig. 2b and c, respectively) produce positional offsets in opposite directions. Early descriptions of induced positional shifts such as these were termed ‘figural after-effects’³⁰.

If the same adaptation-test sequence is repeated for the stimuli shown in Fig. 2b and d, the reader should perceive the offset of the central element in the test stimuli regardless of the orientation of the contrast variations (carrier grating).

To quantify these effects, we generated psychometric functions in which perceived alignment of the central contrast-defined blob was plotted as a function of its true physical position relative to the outer blobs of the test stimulus (Fig. 3). For blobs of increased contrast (contrast increments; open symbols), a substantial leftward (negative) offset of the central blob is required to produce the perception of alignment (that is, prompting 50% rightward responses). For contrast decrements (filled symbols), a rightward offset is required for perceived alignment. Thus, contrast increments and decrements produce perceived shifts of comparable magnitude but opposite directions (although the increment stimuli tend to demonstrate a slightly larger effect). The circles in Fig. 3 indicate cases in

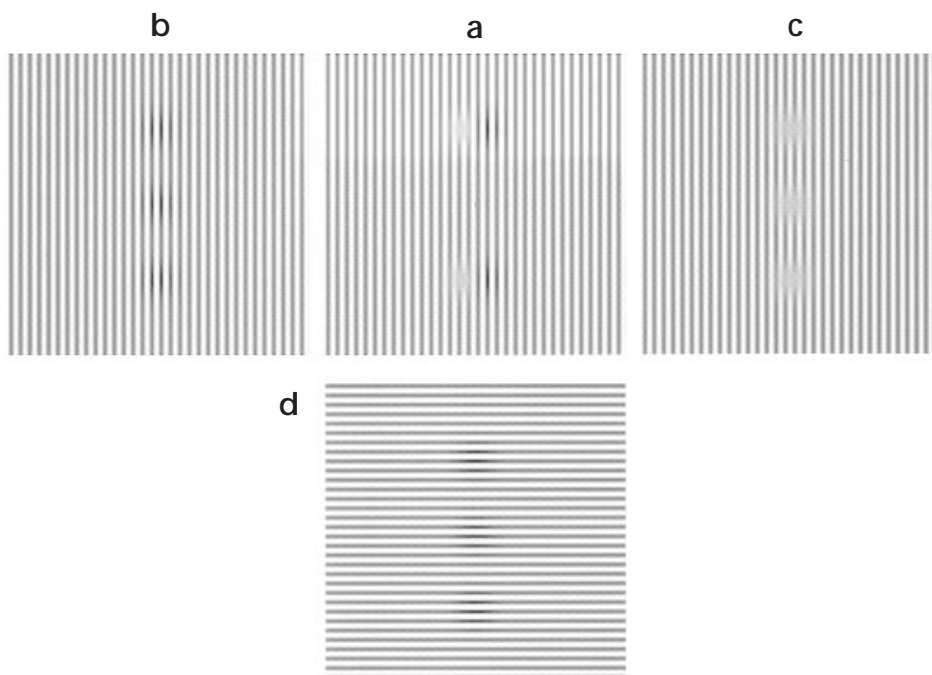


Fig. 2. Demonstration of positional adaptation for second-order stimuli. Prior adaptation to **(a)** again should produce a perceived shift when gaze is transferred to either **(b)** or **(c)**. As with the first-order stimuli, contrast increments and decrements produce shifts in opposite directions. If the reader repeats the process, this time adapting to **(a)** and testing with **(b)** or **(d)**, the magnitude of the perceived offset should be similar for both test stimuli, even though the carrier orientation of the test stimulus in **(d)** is horizontal whereas that of the adapting stimulus is vertical. (Note that because of reproduction non-linearities, some luminance variations may be present in these second-order stimuli.)

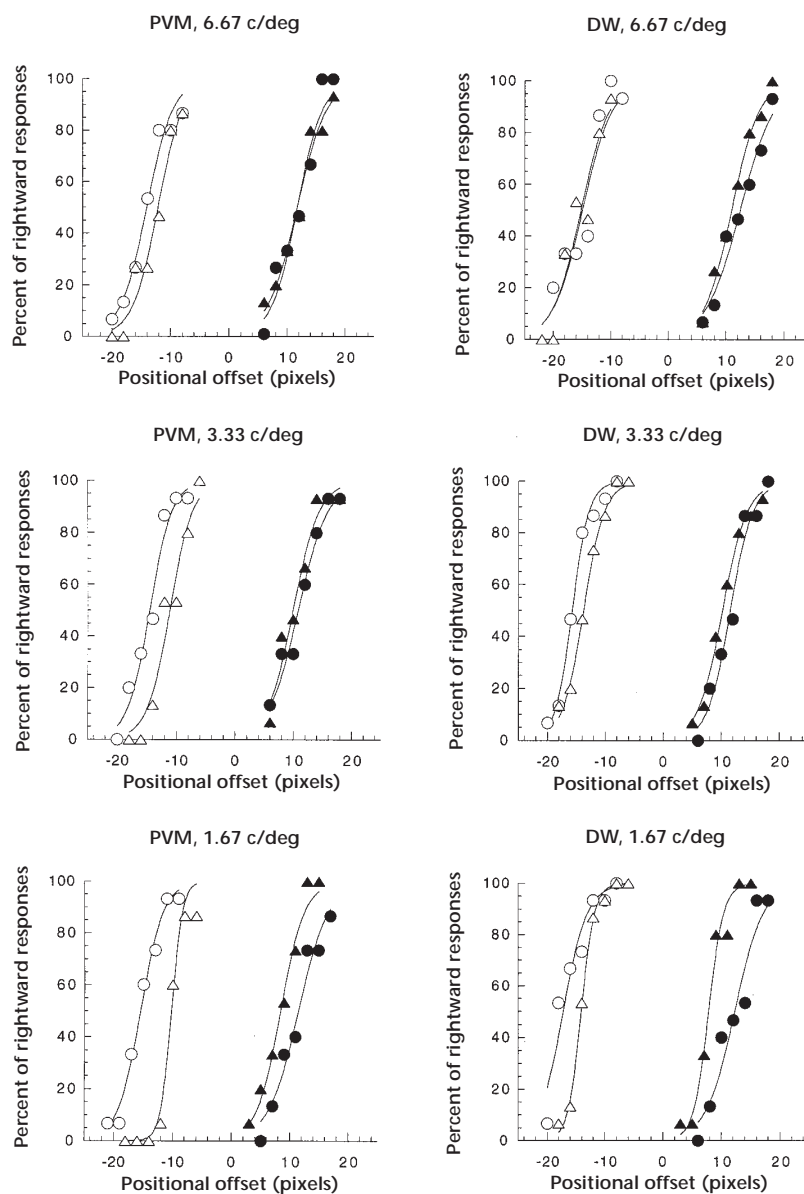


Fig. 3. Orientation crossover at three different carrier spatial frequencies. Circles represent data for which the adapting and test carrier gratings had the same orientation. Triangles represent responses to test gratings whose orientation was orthogonal to that of the adapting stimulus. Open symbols represent contrast increments and filled symbols, contrast decrements.

which carrier gratings for the adapting and test stimuli were of the same orientation (for example, adapting, Fig. 2a; testing, Fig. 2b). Triangles indicate cases in which the grating for the test stimulus was perpendicular to that of the adapting stimulus (for example, adapting, Fig. 2a; testing, Fig. 2d). Perceived shifts for perpendicular and for identically oriented pairs of adapting and test stimuli are similar in magnitude, indicating that there is almost complete crossover of the adaptation effect across different orientations. The amount of orientation crossover reduces slightly as spatial frequency of both adapting and test stimuli are reduced (Fig. 3). For contrast increments, the highest degree of crossover (86.5% for PVM and 98.3% for

DW) is found for a carrier frequency of 6.67 cycles per degree. The amount of orientation crossover is slightly reduced (66% for PVM and 81.9% for DW) for the lowest carrier frequency of 1.67 cycles per degree. Data for contrast decrements show a similar trend, with orientation crossover dropping slightly between the highest carrier frequency (99% for PVM and 88.2% for DW) and the lowest carrier frequency (73.4% for PVM and 63.5% for DW).

Although position adaptation transfers across orientations, it is quite selective for spatial frequency (Fig. 4). When different spatial frequencies are used for the test and adapting carrier gratings, the perceived offset is reduced in magnitude. The circular symbols in Fig. 4 represent cases where the adapting and test stimuli are of the same spatial frequency, the triangular symbols a twofold difference (one octave) and the square symbols a fourfold difference (two octaves). Note that the psychometric functions converge, indicating reduction in effect of adaptation as the difference in spatial frequency becomes greater.

Manipulation of the spatial frequencies of both the adapting and test carrier gratings allows us to plot the magnitude of the effect as a function of spatial frequency difference (Fig. 5). Data are presented for both contrast increments (open columns) and contrast decrements (filled columns). With increasing spatial frequency difference, the magnitude of the perceived offset is reduced, regardless of whether the adapting frequency is higher or lower than the test frequency.

From these data, we calculated for each observer the spatial frequency difference that produced half-maximal adaptation (Table 1). This provides an estimate of the spatial frequency bandwidths of the underlying neural mechanisms, and allows us to compare our psychophysical data with neurophysiological estimates of spatial frequency selectivity³¹. The relevant comparison is with neurons that respond to second-order stimuli, and specifically, with their spatial frequency selectivity for the underlying carrier grat-

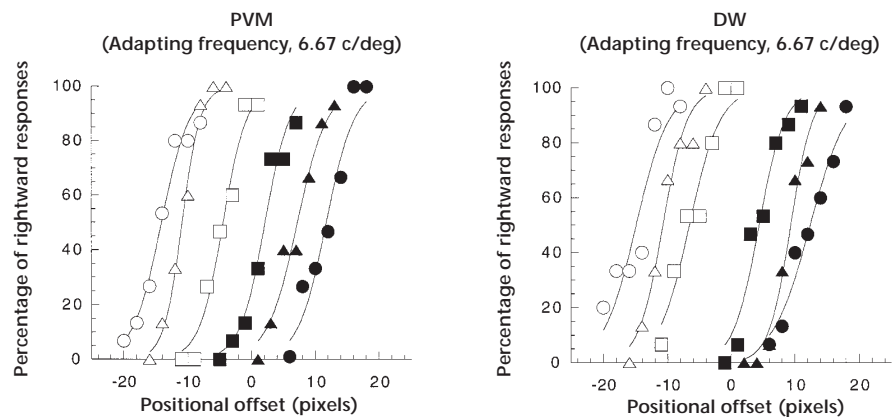
ing. For both observers, spatial frequency bandwidths resulting from contrast increments were somewhat wider than those from contrast decrements; nevertheless, values were comparable to those measured in area 18 of cat visual cortex (mean bandwidth, 1.39 ± 0.86 octaves).

DISCUSSION

We have shown that adaptation to second-order visual stimuli transfers across different orientations, but not across different spatial frequencies. Our results were obtained by psychophysical methods in human subjects, but they correspond closely to neurophysiological findings in visual area 18 of the cat. We found

articles

Fig. 4. Spatial frequency crossover. For circles, adapting and test stimuli had identical spatial frequencies (6.67 cycles per degree). Triangles and squares reflect spatial frequency differences of one octave and two octaves, respectively, between the adapting and test stimuli. Open symbols represent contrast increments and filled symbols, contrast decrements.



that adaptation was specific to a narrow range of carrier frequencies, comparable to the range found for individual cortical neurons that respond to second-order stimuli³¹. The lack of orientation selectivity found in humans might seem to contradict the observation²² that individual area 18 neurons are tuned not only for the orientation of the second-order stimulus but also for the orientation of the underlying first-order carrier stimulus. This can easily be explained, however, if we assume that the psychophysical results reflect the output of a population of such neurons. There seems to be no fixed relationship between the orientation preferences of the second-order filters and their first-order inputs²². Thus, a population of neurons sharing the same second-order orientation preference will receive inputs from first-order filters of all possible orientations, consistent with our observations.

We therefore propose the following model for the detection of second-order information in cat area 18 and in its human cortical equivalent, area V2. Image characteristics are first processed by frequency- and orientation-selective first-order neurons. The outputs from a discrete range of orientations are processed in a non-linear step, which produces the input for a second-order neuron. This neuron has a larger receptive field, and is tuned to a coarser spatial scale than its inputs; it is selective for second-order stimuli of specific orientation, defined by component elements whose orientations are within the range

of the first-order input neurons. Finally, outputs of second-order filters with the same orientation selectivity are pooled, allowing the transfer of positional information across orientation before a localization decision is made. This pooling stage represents the only level at which interaction can occur among second-order stimuli whose contrast variations differ widely in orientation. The finding among the adaptation process is specific with respect to spatial frequency suggests that a similar filtering and pooling process occurs in parallel over many different spatial scales.

Our results are not directly predicted by the well-known phenomenon of contrast adaptation, which involves mechanisms selective for both orientation and spatial frequency²⁴. One possible explanation for the orientation crossover effect would be the presence of an early non-linearity that produces visible distortion products at the initial stages of visual processing (power at frequencies and orientations that are not present in the original image)³². This would provide a possible route of interaction among stimuli that differ widely in their orientation and frequency characteristics³³⁻³⁵. Specifically, if a non-linearity were to render the stimuli visible to neurons early in the visual pathway (neurons with circularly symmetric receptive fields that respond equally to all orientations), this could in principle account for our findings. However, control experiments indicate that this is unlikely to be the case. First,

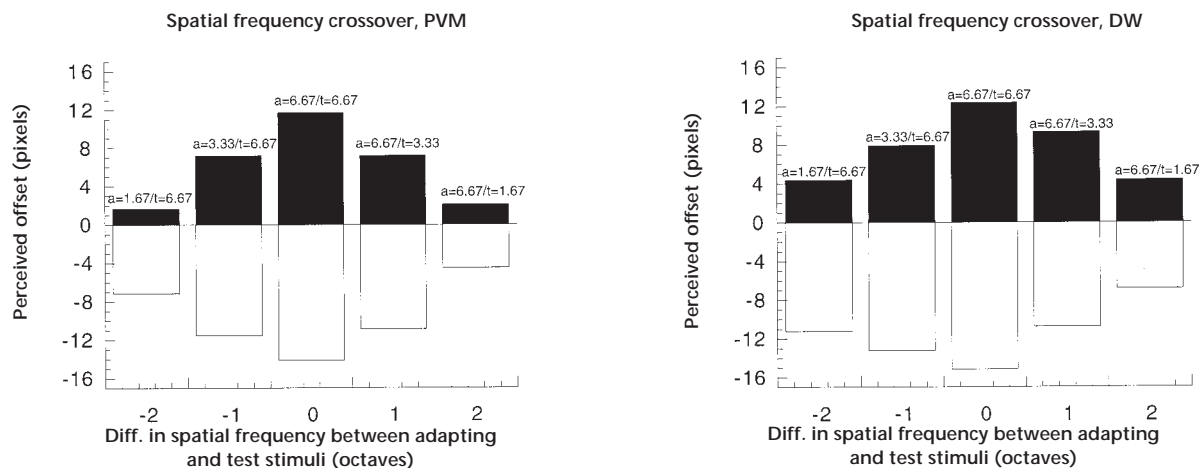


Fig. 5. Spatial frequency bandwidths for positional adaptation. The filled columns represent data for decrements in contrast; the open columns, increments in contrast.

significant positional offsets can be produced at low contrasts (early non-linear distortions may become significant only at high contrasts³⁵), and they continue to demonstrate almost complete transfer across orientation. Second, if adapting and test stimuli were presented to different eyes, we still found significant positional offsets and almost complete orientation crossover. Such an effect could be mediated only by binocular cortical neurons. In contrast, adaptation to first-order information shows little inter-ocular transfer because of the retinal origin of the aftereffect²⁹. Taken together, these results indicate that sensitivity to second-order stimuli is not simply a byproduct of linear processing, but reflects the activity of a dedicated pathway in the visual cortex.

Many models of localization use pooling of first-order filters to explain the acute positional sensitivity of the human visual system^{36,37}. The pooling stage incorporated in the present model of second-order visual processing can therefore be thought of as a scaled version of a process that occurs within the first-order processing stream. Pooling of orientation information may be important in a number of other spatial tasks^{38–41}. For example, human perception of borders between regions composed of differently oriented line elements cannot be accounted for by the independent action of orientation-selective channels, but is readily explained by non-specific pooling of oriented-filter outputs^{40,41}. Although much of the support for orientation pooling is derived from computational modeling⁴⁰ and psychophysical investigations^{39,41}, there are also some indirect physiological correlates. Responses of macaque monkey MT cells to moving contrast-defined bars are largely independent of whether contrast variations of the bar are parallel or perpendicular to the contrast variations of the background²⁰. Together, this evidence suggests that, whereas orientation pooling may occur in the primary visual cortex, it is maintained as a functional characteristic of processing in higher visual centers. The pooling of orientation information represents an efficient method of analyzing objects defined by second-order information. Rather than maintaining a series of localization streams, each tuned to different first-order orientations, pooling of filter outputs before localization allows a single stream to analyze all orientations.

METHODS

Stimuli. A three-element Vernier alignment test stimulus was used in which the observer was required to judge the horizontal location of the central element with respect to the two vertically separated reference elements (see Fig. 2b and c). The center-to-center vertical separation between elements was 2.4°. The stimuli consisted of symmetric Gaussian-windowed contrast modulations (increments and decrements) of a carrier grating whose mathematical description is given by

$$L_{\text{mean}} + \left[\frac{L_{\text{mean}} \sin(2\pi Fx)}{2} \times (1 \pm \text{contrast} \times \exp\left(\frac{-(x^2+y^2)}{2\sigma^2}\right)) \right] \quad (1)$$

where L_{mean} is the mean luminance of the background, σ is the standard deviation of the Gaussian envelope (which was 0.4°), x and y are the horizontal and vertical distances, respectively, from the peak of the contrast envelope and F is the spatial frequency of the carrier grating. Unless otherwise stated, a contrast of 84% was used.

Before presentation of the test stimulus, observers adapted to an anti-symmetric contrast modulation of a carrier grating (first derivative of a Gaussian in the x -direction; Fig. 2a). The mathematical description of these stimuli is given by

Table 1. Magnitude of perceived offsets and spatial frequency bandwidths at half height for contrast increments and decrements (mean \pm s.e.).

	PVM	DW
Decrement peak height (pixels)	11.62 \pm 0.20	11.50 \pm 1.02
Increment peak height (pixels)	-14.07 \pm 0.89	-14.21 \pm 1.47
Decrement width at half height (octaves)	1.22 \pm 0.02	1.83 \pm 0.24
Increment width at half height (octaves)	1.77 \pm 0.16	2.50 \pm 0.57

$$L_{\text{mean}} + \left[\frac{L_{\text{mean}} \sin(2\pi Fx)}{2} \times \left(1 + \text{contrast} \times \exp\left(\frac{-(x^2+y^2)}{2\sigma^2}\right) \times \left(x \frac{\exp(0.5)}{\sigma} \right) \right) \right] \quad (2)$$

All stimuli were generated using the macro capabilities of NIH Image 1.61 public-domain software (available from zippy.nimh.nih.gov by ftp or from the National Technical Information service, Springfield, Virginia, part number PB95-500195GEI) and presented on a 17-inch Apple multiple-scan display with a mean luminance of 34.5 cd per m² and a frame rate of 72 Hz. The non-linear luminance response of the display was corrected using standard photometric procedures. The host computer was a Power Macintosh 7200/90.

Procedure. Observers fixated the center of the adapting stimulus for a period of 5 s (Fig. 2a), immediately followed by a 180-ms exposure to the test stimulus (Fig. 2b and c). Fixation remained constant, such that the outer elements of the test stimulus were presented in the same retinal location as the adapting stimulus. The adapting stimulus was counter-phased at one Hz to avoid retinal after-image formation. All tests were done under dim room illumination. The spatial frequency (6.67, 3.33 or 1.67 cycles per degree) and orientation (vertical or horizontal) of the carrier grating were varied in both the adapting and test stimuli. The magnitude of the perceived offset in the test stimulus following adaptation was established using a method of constant stimuli. One of seven values of central element offset was presented in each trial, with the midpoint of these values approximating subjective alignment as determined by pilot experiments. A step size of two pixels (3.2 arcmin) between each of the seven offsets produced an appropriate range of responses from approximately 100% rightward to 100% leftward. To allow the adaptation effect to plateau, the results of the first 20 trials were discarded. Subsequently, 20 trials were presented at each of the 7 offsets and the proportion of "rightward" responses was calculated for each offset. The resulting data were fitted with a logistic function of the form

$$y = \frac{100}{1 + e^{-\frac{(x-\mu)}{\theta}}}$$

where μ is the offset corresponding to the 50% level on the psychometric function (perceived alignment), and θ provides an estimate of alignment threshold (approximately half the offset between the 27% and 73% levels on the psychometric function).

ACKNOWLEDGEMENTS

P.V.M. is supported by a Vision Research Training Fellowship from the Wellcome Trust. D.M.L. is supported by grant RO1EY01728 from the National Eye Institute, NIH, Bethesda, Maryland.

RECEIVED 11 JANUARY; ACCEPTED 1 MARCH 1999

- Hubel, D. H. & Wiesel, T. N. Receptive fields, binocular interaction, and functional architecture in the cat's visual cortex. *J. Physiol. (Lond.)* **160**, 106–154 (1962).
- Movshon, J. A., Thompson, I. A. & Tollhurst, D. J. Spatial summation in the receptive fields of simple cells in the cat's striate cortex. *J. Physiol. (Lond.)* **283**, 53–77 (1978).
- Spitzer, H. & Hochstein, S. Simple- and complex-cell response dependences on stimulation parameters. *J. Neurophysiol.* **53**, 1244–1265 (1985).

4. Shapley, R. M. & Lennie, P. Spatial frequency analysis in the visual system. *Annu. Rev. Neurosci.* **8**, 547–583 (1985).
5. von der Heydt, R. & Peterhans, E. Mechanisms of contour perception in monkey visual cortex. I. Lines of pattern discontinuity. *J. Neurosci.* **9**, 1731–1748 (1989).
6. von der Heydt, R., Peterhans, E. & Dursteler, M. R. Periodic-pattern-selective cells in monkey visual cortex. *J. Neurosci.* **12**, 1416–1434 (1992).
7. Merigan, W. H., Nealey, T. A. & Maunsell, J. H. Visual effects of lesions of cortical area V2 in macaques. *J. Neurosci.* **13**, 3180–3191 (1993).
8. Shapley, R. M. Visual cortex: pushing the envelope. *Nat. Neurosci.* **1**, 95–96 (1998).
9. Li-Ming, L. & Wilson, H. R. Fourier and non-Fourier pattern discrimination. *Vision Res.* **36**, 1907–1918 (1996).
10. Chubb, C. & Sperling, G. Drift-balanced random stimuli: A general basis for studying non-Fourier motion perception. *J. Opt. Soc. Am. A* **5**, 1986–2007 (1988).
11. Turano, K. & Pantle, A. On the mechanism that encodes the movement of contrast variations: Velocity discrimination. *Vision Res.* **29**, 207–221 (1974).
12. Derrington, A. M., Badcock, D. R. & Henning, G. B. Discriminating the direction of second-order motion at short stimulus durations. *Vision Res.* **33**, 1785–1794 (1993).
13. Ledgeway, T. & Smith, A. T. Evidence for separate motion-detecting mechanisms for first- and second-order motion in human vision. *Vision Res.* **34**, 2727–2740 (1994).
14. Vaina, L. M., Makris, N., Kennedy, D. & Cowey, A. The selective impairment of the perception of first-order motion by unilateral brain damage. *Vis. Neurosci.* **15**, 333–348 (1998).
15. Zhou, Y.-X. & Baker, C. L. A processing stream in mammalian visual cortex neurons for non-Fourier responses. *Science* **261**, 98–101 (1993).
16. Morgan, M. J. & Hotopf, W. H. Perceived diagonals in grids and lattices. *Vision Res.* **29**, 1005–1015 (1989).
17. Victor, J. D. & Conte, M. M. Spatial organization of nonlinear interactions in form perception. *Vision Res.* **31**, 1457–1488 (1991).
18. Graham, N., Beck, J. & Sutter, A. Nonlinear processes in spatial-frequency channel models of perceived texture segregation: effects of sign and amount of contrast. *Vision Res.* **32**, 719–743 (1992).
19. Levi, D. M. & Waugh, S. J. Position acuity with opposite-contrast polarity features: evidence for a nonlinear collector mechanism for position acuity. *Vision Res.* **36**, 573–588 (1996).
20. Olavarria, J. F., DeYoe, E. A., Knierim, J. J., Fox, J. M. & Van Essen, D. C. Neural responses to visual texture patterns in the middle temporal area of the macaque monkey. *J. Neurophysiol.* **68**, 164–181 (1992).
21. Shapley, R. M. in *Higher-Order Processing in the Visual System. Ciba Foundation Symposia* 71–87 (Wiley, New York, 1994).
22. Mareschal, I. & Baker, C. L. A cortical locus for the processing of contrast-defined contours. *Nat. Neurosci.* **1**, 150–154 (1998).
23. Pantle, A. & Sekuler, R. Size detecting mechanisms in human vision. *Science* **162**, 1146–1148 (1968).
24. Blakemore, C. & Campbell, F. W. On the existence of neurons in the human visual system selectively sensitive to the orientation and size of retinal images. *J. Physiol. (Lond.)* **203**, 237–260 (1969).
25. Gibson, J. J. & Radner, M. Adaptation, aftereffect, and contrast in the perception of tilted lines. I. Quantitative studies. *J. Exp. Psychol.* **20**, 453–467 (1937).
26. Moulden, B., Renshaw, J. & Mather, G. Two channels for flicker in the human visual system. *Perception* **13**, 387–400 (1984).
27. McCollough, C. Color adaptation of edge detectors in the human visual system. *Science* **149**, 1113–1114 (1965).
28. Pantle, A. Motion aftereffect magnitude as a measure of spatiotemporal response properties of direction-selective analysers. *Vision Res.* **14**, 1229–1236 (1974).
29. Whitaker, D., McGraw, P. V. & Levi, D. M. The influence of adaptation on perceived visual location. *Vision Res.* **37**, 2207–2216 (1997).
30. Sutherland, N. S. Figural after-effects and apparent size. *J. Exp. Psychol.* **13**, 222–228 (1961).
31. Mareschal, I. & Baker, C. L. Temporal and spatial response to second-order stimuli in cat area 18. *J. Neurophysiol.* **80**, 2811–2823 (1998).
32. Burton, G. J. Evidence for non-linear response process in the visual system from measurements on the thresholds of spatial beat frequencies. *Vision Res.* **13**, 1211–1255 (1973).
33. Henning, G. B., Hertz, G. B. & Broadbent, D. E. Some experiments bearing on the hypothesis that the visual system analyses patterns in independent bands of spatial frequency. *Vision Res.* **15**, 887–897 (1975).
34. Nachmias, J. N. & Rogowitz, B. E. Masking by spatially modulated gratings. *Vision Res.* **23**, 1621–1629 (1983).
35. Derrington, A. M. & Badcock, D. R. Detecting spatial beats: non-linearity or contrast increment detection? *Vision Res.* **27**, 343–348 (1986).
36. Klein, S. A. & Levi, D. M. Hyperacuity thresholds of 1 sec: Theoretical predictions and empirical validation. *J. Opt. Soc. Am. A* **2**, 1170–1190 (1985).
37. Wilson, H. R. Responses of spatial mechanisms can explain hyperacuity. *Vision Res.* **26**, 453–469 (1986).
38. Georgeson, M. A. Human vision combines oriented filters to compute edges. *Proc. R. Soc. Lond. B* **249**, 235–245 (1992).
39. Thomas, J. P. & Olzak, L. A. Uncertainty experiments support the roles of second-order mechanisms in spatial frequency and orientation discriminations. *J. Opt. Soc. Am. A* **13**, 689–696 (1996).
40. Nothdurft, H. C. in *Structural and Functional Organization of the Neocortex* (eds Albus, K., Kuhnt, U., Nothdurft, H. C. & Wahle, P.) 375–384 (Springer, Berlin, 1994).
41. Sagi, D. in *Early Vision and Beyond* (eds Pappas, T. V., Chubb, C., Gorea, A. & Kowler, E.) 69–78 (MIT Press, Cambridge, Massachusetts, 1995).